BIOCHEMISTRY
including biophysical chemistry & molecular biology
Article

Biochemistry **2010,** *49,* 9985–9996 9985
DOI: 10.1021/bi101023c

Biotin Synthase Exhibits Burst Kinetics and Multiple Turnovers in the Absence of Inhibition by Products and Product-Related Biomolecules†

Christine E. Farrar,‡ Karen K. W. Siu,§,∥ P. Lynne Howell,§,∥ and Joseph T. Jarrett*,‡

‡*Department of Chemistry, University of Hawaii at Manoa, Honolulu, Hawaii 96822, United States,* §*Program in Molecular Structure and Function, Research Institute, The Hospital for Sick Children, 555 University Avenue, Toronto, Ontario M5G 1X8, Canada, and* ∥*Department of Biochemistry, University of Toronto, Toronto, Ontario M5S 1A8, Canada*

Received June 25, 2010; Revised Manuscript Received October 15, 2010

ABSTRACT: Biotin synthase (BS) is a member of the "SAM radical" superfamily of enzymes, which catalyze reactions in which the reversible or irreversible oxidation of various substrates is coupled to the reduction of the *S*-adenosyl-L-methionine (AdoMet) sulfonium to generate methionine and 5′-deoxyadenosine (dAH). Prior studies have demonstrated that these products are modest inhibitors of BS and other members of this enzyme family. In addition, the *in vivo* catalytic activity of *Escherichia coli* BS requires expression of 5′-methylthioadenosine/*S*-adenosyl-L-homocysteine nucleosidase, which hydrolyzes 5′-methylthioadenosine (MTA), *S*-adenosyl-L-homocysteine (AdoHcy), and dAH. In the present work, we confirm that dAH is a modest inhibitor of BS (K_i = 20 μM) and show that cooperative binding of dAH with excess methionine results in a 3-fold enhancement of this inhibition. However, with regard to the other substrates of MTA/AdoHcy nucleosidase, we demonstrate that AdoHcy is a potent inhibitor of BS ($K_i \leq$ 650 nM) while MTA is not an inhibitor. Inhibition by both dAH and AdoHcy likely accounts for the *in vivo* requirement for MTA/AdoHcy nucleosidase and may help to explain some of the experimental disparities between various laboratories studying BS. In addition, we examine possible inhibition by other AdoMet-related biomolecules present as common contaminants in commercial AdoMet preparations and/or generated during an assay, as well as by sinefungin, a natural product that is a known inhibitor of several AdoMet-dependent enzymes. Finally, we examine the catalytic activity of BS with highly purified AdoMet in the presence of MTAN to relieve product inhibition and present evidence suggesting that the enzyme is half-site active and capable of undergoing multiple turnovers *in vitro*.

Biotin synthase (BS)[1] is an *S*-adenosyl-L-methionine (AdoMet) radical enzyme (*1*−*6*) that catalyzes the oxidative addition of a sulfur atom to dethiobiotin (DTB), generating the biotin thiophane ring (*3*−*5*, *7*, *8*). The reaction sequence is initiated by the reductive cleavage of AdoMet, yielding methionine and a transient 5′-deoxyadenosyl carbon radical (dA·). This high-energy radical functions as an oxidant, abstracting a hydrogen atom from the C9 methyl group of DTB, producing 5′-deoxyadenosine (dAH) and a putative dethiobiotinyl carbon radical (*1*, *3*, *9*). The radical chain reaction is quenched by the addition of a sulfur atom, most likely derived from a nearby $[2Fe\text{-}2S]^{2+}$ cluster, generating 9-mercaptodethiobiotin (MDTB) (*6*, *9*, *10*). A similar reaction sequence with a second equivalent of AdoMet results in abstraction of the C6 methylene pro-*S* hydrogen atom from MDTB (*1*, *3*, *11*), and the resulting carbon radical is quenched via formation of an intramolecular C−S bond, thus closing the biotin thiophane ring. *In vitro*, biotin production is accompanied by loss of the $[2Fe\text{-}2S]^{2+}$ cluster (*12*−*14*), resulting in apparent inactivation of the enzyme following a single turnover. *In vivo*, the $[2Fe\text{-}2S]^{2+}$ cluster is likely reassembled by members of the Isc or Suf iron−sulfur cluster assembly systems (*15*, *16*), sustaining multiple catalytic turnovers over several hours (*17*).

Like most members of the AdoMet radical (or "radical SAM") superfamily, BS couples the irreversible reductive cleavage of AdoMet to oxidation of the substrate and is therefore using AdoMet as a stoichiometric substrate rather than as a cofactor (*18*, *19*). *In vitro*, BS also catalyzes the uncoupled reductive cleavage of AdoMet to varying degrees depending on the reaction conditions (*2*−*4*, *6*). Prior studies suggest that the conversion of 1 equiv of DTB to biotin as catalyzed by *Escherichia coli* BS is coupled to the production of 2.2−4 equiv of the AdoMet-derived products dAH and methionine (*1*−*6*), with 2 equiv presumably produced by the enzymatic reaction and the remainder produced by uncoupled reductive cleavage.

It is perhaps not surprising that BS is subject to product inhibition. Fontecave and co-workers first demonstrated that dAH is an inhibitor of BS, with 30 μM dAH resulting in ∼90% inhibition of biotin production in a 90 min assay (*20*). Roach and co-workers also demonstrated that *E. coli* BS, as well as the AdoMet radical enzymes *E. coli* tyrosine lyase (ThiH) and *Sulfolobus solfataricus* lipoyl synthase (LipA), is inhibited by dAH and methionine (*21*). BS was reported to be inhibited by dAH alone with an $IC_{50} \approx$ 400 μM and by a 1:1 mixture of dAH and methionine with an IC_{50} = 114 ± 14 μM. It should be noted that these assays used a high concentration of AdoMet, which would increase the observed IC_{50}. In addition, the assays were conducted for 3 h at 37 °C, a time at which the production of biotin has slowed and significant amounts of additional dAH and Met have been

†This research has been supported by grants from the National Science Foundation (MCB 09-23829 to J.T.J.) and the Canadian Institutes of Health Research (no. 43998 to P.L.H.).

*Correspondence should be directed to this author. Phone: 808-956-6721. Fax: 808-956-5908. E-mail: jtj@hawaii.edu.

[1]Abbreviations: AdoMet, *S*-adenosyl-L-methionine; AdoHcy, *S*-adenosyl-L-homocysteine; Aib, 2-aminoisobutyric acid; BS, *Escherichia coli* biotin synthase (BioB); dAH, 5′-deoxyadenosine; dA·, 5′-deoxyadenosyl radical; DTB, dethiobiotin; DTT, dithiothreitol; ESI MS, electrospray ionization mass spectrometry; MDTB, 9-mercaptodethiobiotin; MTA, 5′-methylthioadensine; MTAN, 5′-methylthioadenosine/*S*-adenosyl-L-homocysteine nucleosidase; PFL, pyruvate formate-lyase; Tris, tris(hydroxymethyl)aminomethane.

Published on Web 10/20/2010

generated, and therefore the data may underestimate the true inhibition constants. Choi-Rhee and Cronan first reported that dAH is cleaved by 5′-methylthioadenosine/*S*-adenosyl-L-homocysteine nucleosidase (MTAN, referred to as Pfs by Choi-Rhee and Cronan and in other prior studies), producing adenine and presumably 5-deoxyribose (*22*). Roach and co-workers also report that dAH is an alternate substrate for MTAN and that addition of this enzyme to BS assays mostly relieves dAH product inhibition (*21*). *In vivo* studies by Choi-Rhee and Cronan demonstrated that de novo biotin biosynthesis in *E. coli* is suppressed by mutation of the *pfs* gene (now referred to as *mtn*). Since a secondary mutation of *speE* (spermidine synthase), the predominant source of MTA in *E. coli*, did not restore growth in the absence of biotin, MTA was ruled out as an inhibitor of BS, and it was hypothesized that *in vivo* inhibition of BS was caused by a buildup of the BS product dAH (*22*).

In the present work, inhibition of BS by products and by several product-related biomolecules was further investigated. Initial studies suggested that a contaminant in commercial AdoMet preparations was acting as a potent but highly variable inhibitor; further studies were carried out with ≥93% pure (*S*,*S*)-AdoMet freshly prepared using *E. coli* AdoMet synthetase. A quick inhibition screen was then used to identify biomolecules that inhibited with $IC_{50} \leq 500\ \mu M$. Further detailed inhibition studies with AdoHcy and sinefungin were fit to an interacting-monomer dimeric enzyme inhibition model to yield relatively precise kinetic constants: $K_m^{AdoMet} = 10\ \mu M$, $K_i^{AdoHcy} = 650$ nM, $K_i^{sinefungin} = 75\ \mu M$, and k_{cat} initial = 0.042 min^{-1}. In addition, the individual and cooperative inhibitory effects of dAH and methionine were examined, yielding inhibition constants for dAH alone, $K_i^{dAH} = 20\ \mu M$, and for dAH in the presence of saturating methionine, $K_i^{dAH:Met} = 6\ \mu M$. Finally, an optimized time course for the catalytic activity of BS, in the presence of MTAN to relieve dAH and AdoHcy inhibition, reveals that the enzyme appears to undergo burst kinetics followed by three to four additional slower turnovers, and this conjecture is supported by ESI MS studies demonstrating delayed incorporation of ^{34}S-sulfide from the buffer into biotin. Perhaps most surprising, a careful stoichiometric analysis of the inhibition and kinetic data suggests that the BS dimer may exhibit half-site reactivity, in which the one monomer turns over at a rate at least an order of magnitude faster than the second monomer.

MATERIALS AND METHODS

Materials. Except where otherwise specified, reagents were purchased from commercial sources and used without further purification. Commercial AdoMet, AdoHcy, MTA, adenine, and dAH were purchased from Sigma, and stock solution concentrations were determined using $\varepsilon_{260} = 13600\ M^{-1}\ cm^{-1}$ at pH 7. MTAN was purified as previously described (*23*). A codon-optimized synthetic gene encoding *E. coli* BS (GenScript) was ligated into pET21d with an additional N-terminal hexahistidine tag sequence, and the plasmid was transformed into BL21(DE3)pLysS (Novagen). His_6-BS was then prepared as previously described (*14*), and the hexahistidine tag was not removed. The synthetic gene construct was designed to maintain the identical protein sequence as our prior N-terminal hexahistidine-tagged protein (*24*), but the codon-optimized plasmid produces ca. 3 times more protein than prior constructs, yielding ~100 mg of protein/L of bacterial culture. The concentration of aerobically purified BS was estimated based on the absorbance spectrum of the $[2Fe\text{-}2S]^{2+}$ cluster using $\varepsilon_{452} = 8400\ M^{-1}\ cm^{-1}$ and confirmed by the Bradford assay using BSA as a standard (*25*).

Enzymatic Preparation of AdoMet. The strain DM22-(pK8) that overproduces AdoMet synthetase (*26*, *27*) was initially constructed by Dr. G. D. Markham (Fox Chase Cancer Center) and was a gift to our laboratory from Dr. J. Broderick (Montana State University). AdoMet synthetase cell-free lysate (~15 mg/mL crude protein) was prepared as previously described (*28*−*30*). AdoMet was synthesized using a modification of a previously described procedure (*30*). Briefly, a cell-free lysate prepared from DM22(pK8) (10 mL, 150 mg of crude protein) was mixed with adenosine triphosphate (13 mM) and L-methionine (10 mM) in 100 mM Tris-HCl, 50 mM KCl, 26 mM $MgCl_2$, 1 mM EDTA, and 20% CH_3CN, pH 8.0, and the reaction was stirred at room temperature for 2 h. The reaction mixture was acidified with 10 mL of 4.0 M sodium acetate, pH 4.0, and placed on ice for 15 min. Precipitated protein was removed by centrifugation at 30000*g* for 30 min.

AdoMet was purified by weak cation-exchange chromatography. Approximately 100 mL of clarified supernatant from the reaction above was diluted 1:1 with deionized water, passed through a 0.2 μm filter, and loaded onto Amberlite CG-50 (20 mL) preequilibrated with 0.2 M sodium acetate, pH 4.0. The column was washed with 200 mL of the same buffer, and AdoMet was then eluted from the column with a 200 mL linear gradient from 0 to 0.1 M HCl. Fractions were frozen, lyophilized for ~30 h, and dissolved in sterile deionized water (final pH ≈ 2), and the concentration of the AdoMet was determined by absorbance at 260 nm. A 50 mM stock solution was prepared by dilution with sterile deionized water, aliquotted, and stored at −80 °C. The purity of each fraction was examined by HPLC analysis. Samples were injected on a 3.0 × 150 mm, 5 μm Atlantis dC18 reversed-phase column (Waters) and eluted with 100% solvent A for 8 min, followed by a linear gradient from 0% to 95% solvent B for 10 min, and then 100% solvent B for 7 min (solvent A, 200 mM ammonium acetate; solvent B, 100% methanol) at a flow rate of 0.7 mL/min and a column temperature of 25 °C. AdoMet ($t_R \approx 7$ min), AdoHcy ($t_R \approx 15$ min), and MTA ($t_R \approx 18$ min) were detected at 260 nm.

Standard BS Activity Assay. All materials were transferred into an anaerobic chamber 15 min prior to the start of the assay. BS (25 μM in 200 μL final volume, unless otherwise indicated) was added to 1.5 mL microcentrifuge tubes containing 50 mM Tris-HCl, 100 mM KCl, and 5 mM DTT, pH 8.0. The $[4Fe\text{-}4S]^{2+}$ cluster was reconstituted by incubation with Na_2S (200 μM) and $FeCl_3$ (200 μM) for 5 min. Flavodoxin (25 μM), ferredoxin (flavodoxin):$NADP^+$ oxidoreductase (4 μM), NADPH (1 mM), and DTB (50 μM) were added and the samples incubated for 5 min. Turnover was initiated by the addition of AdoMet (100 μM), and the tubes were sealed, removed from the anaerobic chamber, and incubated in a 37 °C water bath for 30 min. Sodium acetate, pH 4.5 (20 μL of 4.5 M stock), was added to quench the reaction and precipitate the protein. The tubes were incubated on ice for 10 min, the precipitated protein was removed by centrifugation for 10 min at 18000*g*, and the supernatant was transferred to an HPLC autosampler vial. HPLC quantitation of DTB, biotin, dAH, and AdoMet samples was carried out as previously described (*9*).

MTA/AdoHcy Nucleosidase Activity Assay. Nucleosidase activity was quantified by coupling the reaction to a colorimetric xanthine oxidase assay (*31*) as previously described (*32*). Reactions contained *E. coli* MTAN (12 nM), dAH (3−250 μM), xanthine oxidase (0.28 unit), and *p*-iodonitrotetrazolium violet (INT, 1 mM) in 50 mM sodium phosphate, pH 7.5. Xanthine oxidase couples the oxidation of adenine (to 2,8-dihydroxyadenine) to the reduction of 2 equiv of INT to the corresponding formazan. The absorbance at 470 nm was monitored for 10 min

on a Biochrome Ultrospec 2100 UV/vis spectrophotometer. The amount of formazan produced was determined using ε_{470} = 15400 M^{-1} cm^{-1}, and the result was divided by 2 to give the amount of adenine produced. Each substrate concentration was analyzed in triplicate, and K_m and V_{max} values were determined by fitting initial velocity data to the Henri−Michaelis−Menten equation. The formation of adenine as the sole nucleotide product was confirmed by ESI MS.

Determination of Inhibition Constants. Competitive inhibition constants were determined by examining the effect of preincubation with inhibitors on the first turnover of biotin formation, which occurs within the first 30 min after the enzyme is mixed with substrates. As long as both substrate binding (k_{on} ~ 1−100 s^{-1} (*33*)) and inhibitor binding are rapid relative to the rate of biotin formation (~0.001 s^{-1}), i.e., the enzyme is in a rapid equilibrium between free enzyme and substrate- or inhibitor-bound forms, then the pre-steady-state inhibition constants can be determined using steady-state equations, except that V_{max} does not include product release and subsequent steps that might be involved in enzyme recycling. However, the values obtained for K_m and K_i should compare well with the equilibrium dissociation constants for the respective substrates and inhibitors.

To determine inhibition constants, the initial rate of biotin formation was measured while varying the concentration of AdoMet (100−500 μM) in the presence of sinefungin (0−1000 μM) or AdoHcy (0−50 μM). Because BS is a homodimer, there are two active sites to which substrate or inhibitor can bind, and inhibitor bound to one monomer could potentially affect the conformation and activity of the second monomer. Therefore, the inhibition constants were obtained by fitting the data to competitive inhibition involving a cooperative two-site system:

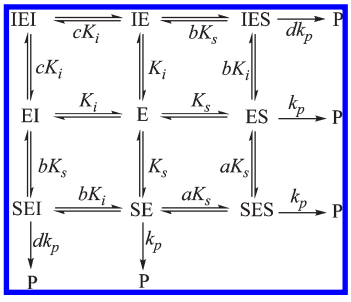

Inhibition constants were then determined by fitting the data to the velocity equation:

$$\frac{v}{V_{max}} = \frac{\frac{[S]}{K_s} + \frac{[S]^2}{aK_s^2} + d\frac{2[S][I]}{bK_sK_i}}{1 + \frac{2[S]}{K_s} + \frac{[S]^2}{aK_s^2} + \frac{2[S][I]}{bK_sK_i} + \frac{2[I]}{K_i} + \frac{[I]^2}{cK_i^2}} \quad (1)$$

where [S] represents the concentration of AdoMet, [I] represents the concentration of inhibitor, *a*, *b*, and *c* are the factors by which the K_s or K_i of the vacant site changes when the first molecule of the AdoMet or AdoHcy binds (binding cooperativity), and *d* is the factor by which the rate of product formation is decreased when both AdoMet and inhibitor are bound to opposing monomers (catalytic cooperativity). This approach is similar to that presented by Segel (*34*), except that we have added an additional term and the factor *d* that accounts for possible partial activity of the mixed IES/SEI complexes.

To determine binding constants for the cooperative product inhibitors, dAH and methionine, BioB activity assays were carried out in duplicate at 37 °C for 30 min with varying concentrations of dAH (50−500 μM) and methionine (200−2000 μM), all at [AdoMet] = 100 μM. The inhibition constants for dAH and methionine were obtained by fitting the data to a general equation for cooperative competitive inhibition by two different nonexclusive inhibitors, which can be expressed in general terms as

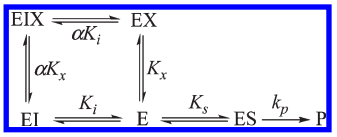

where I and X represent dAH and methionine, respectively, two different inhibitors that bind to BS at different parts of the active site, and the binding of either inhibitor prevents AdoMet from binding. Inhibition constants were then determined by fitting the data to the velocity equation:

$$\frac{v}{V_{max}} = \frac{\frac{[S]}{K_s}}{1 + \frac{[S]}{K_s} + \frac{[I]}{K_i} + \frac{[X]}{K_x} + \frac{[I][X]}{\alpha K_i K_x}} \quad (2)$$

where [S] represents the concentration of AdoMet, [I] and [X] represent the concentration of inhibitors dAH and methionine, K_s is set at 10 μM as determined for data in Figure 3, and α is the cooperativity factor that describes the extent to which the binding of one inhibitor affects the binding of the other within the same active site. We did not need to include cooperativity between separate monomers within the BS dimer to accurately model the data.

Apparent inhibition by a contaminant in commercial AdoMet samples was analyzed using a model for noncompetitive inhibition by a trace contaminant, as described by Segel (*35*). This model can also be applied to cooperative inhibition in a dimeric enzyme when binding of inhibitor to one active site results in noncompetitive loss of activity at the other active site; this scenario is invoked to model inhibition by AdoHcy and sinefungin above and may be attributable to the proposed half-site reactivity as discussed below. The data are fit using the equation:

$$\frac{v}{V_{max}} = \frac{\frac{[S]}{K_s}}{1 + \frac{[S]}{K_s} + \frac{x[S]}{K_i} + \frac{x[S]^2}{K_iK_s}} \quad (3)$$

where [S] represents the concentration of AdoMet and x = [I]/[S] is the fractional level of the impurity causing inhibition. Note that K_i cannot be determined explicitly since the concentration of the inhibitor is unknown; only the ratio x/K_i can be determined.

Determination of the Dissociation Constant for AdoHcy. When AdoMet is added to reconstituted BS containing both $[2Fe\text{-}2S]^{2+}$ and $[4Fe\text{-}4S]^{2+}$ clusters, a small decrease in the UV/visible spectrum at 380−420 nm is observed. Using this spectral change as a probe, the binding constant for AdoMet was previously determined (*33*). In the present study, a similar method was applied for determining the binding constant for AdoHcy in the presence of saturating DTB. Briefly, a solution of BS (50 μM) was preincubated under nitrogen with 50 mM Tris-HCl, 100 mM KCl, pH 8.0, 5 mM DTT, and 200 μM DTB. The $[4Fe\text{-}4S]^{2+}$ cluster was

reconstituted by incubation with Na_2S and $FeCl_3$ (200 μM each) for 5 min. The BS mixture was kept in a septum-covered quartz cuvette as AdoHcy was added by syringe (2 μL of 1 mM stock per addition). After each addition of AdoHcy, the sample was briefly mixed, and its UV/visible spectrum was recorded. The change in the absorbance difference between 400 and 500 nm was examined as a function of added AdoHcy, and the resulting data were fit to a quadratic binding isotherm:

$$\Delta A = \Delta A_\infty \left[\frac{([E] + [S] + K_d) - \sqrt{([E]+[S]+K_d)^2 - 4[E][S]}}{2[E]} \right] \quad (4)$$

where [E] is the concentration of binding sites, [S] is the AdoHcy concentration, and K_d is the dissociation constant for AdoHcy.

Analysis of the Time Dependence of Biotin Formation in the Absence of Inhibition. Since prior studies have routinely been performed with commercial AdoMet that is contaminated with AdoHcy and have routinely ignored possible product inhibition, we performed a time course under optimized conditions in the presence of 100-fold more MTAN than necessary to consume all dAH, MTA, and AdoHcy that might be initially present or produced in the assay. BioB activity assays were performed as described above, except with the following concentrations: BS (22 ± 1 μM monomer), AdoMet (200 μM), DTB (200 μM), and MTAN (200 nM). Samples were quenched at various time points from 10 min to 4 h, and the concentration of products was measured by HPLC. Data were fit to an equation with an exponential burst phase followed by a linear steady-state phase:

$$[P] = [E]((1 - e^{-k_{burst}}) + k_{SS}t) \quad (5)$$

where [P] is the observed concentration of the product biotin or dAH, [E] is the concentration of enzyme active sites participating in the burst, k_{burst} is the observed rate constant for the burst phase, and k_{SS} is the turnover number for the steady-state phase.

Mass Spectrometry. The mass of biotin was determined by HPLC coupled to an Agilent 6210 TOF ESI mass spectrometer. The HPLC separation for biotin was performed on an Agilent 1100 series liquid chromatography system equipped with a 2.1 mm × 150 mm, 5 μm Atlantis dC18 reversed-phase column (Waters) using a 25 min linear gradient from 100:0 to 75:25 H_2O:acetonitrile (both containing 0.1% (v/v) formic acid) at a flow rate of 0.7 mL/min. ESI MS parameters were as follows: positive ion mode; nitrogen was used as the nebulizer drying gas (pressure, 30 psi; flow rate, 10 L/min; temperature, 325 °C); spray capillary voltage, 3500 V; skimmer voltage, 65 V; fragmenter voltage, 175 V; OctRFV voltage, 250 V. Mass spectra were acquired over the range m/z = 150−1000 at a scan speed of 0.99 scan/s. MassHunter Workstation Software v B.02.00 (Agilent) was used for instrument control, data acquisition, and data analysis.

RESULTS

Biotin Synthase Is Inhibited by Contaminants in Commercial AdoMet. Prior studies had suggested that dAH, and perhaps other AdoMet-related biomolecules, could act as competitive inhibitors of BS activity. In order to quantitatively analyze the inhibition of BS by potential competitive inhibitors, we needed to obtain a reliable value for the K_m for AdoMet. We conducted assays at varying AdoMet concentrations using commercially available AdoMet (purchased as the iodide and *p*-toluenesulfonate salts from Sigma) and unexpectedly obtained data that suggested that

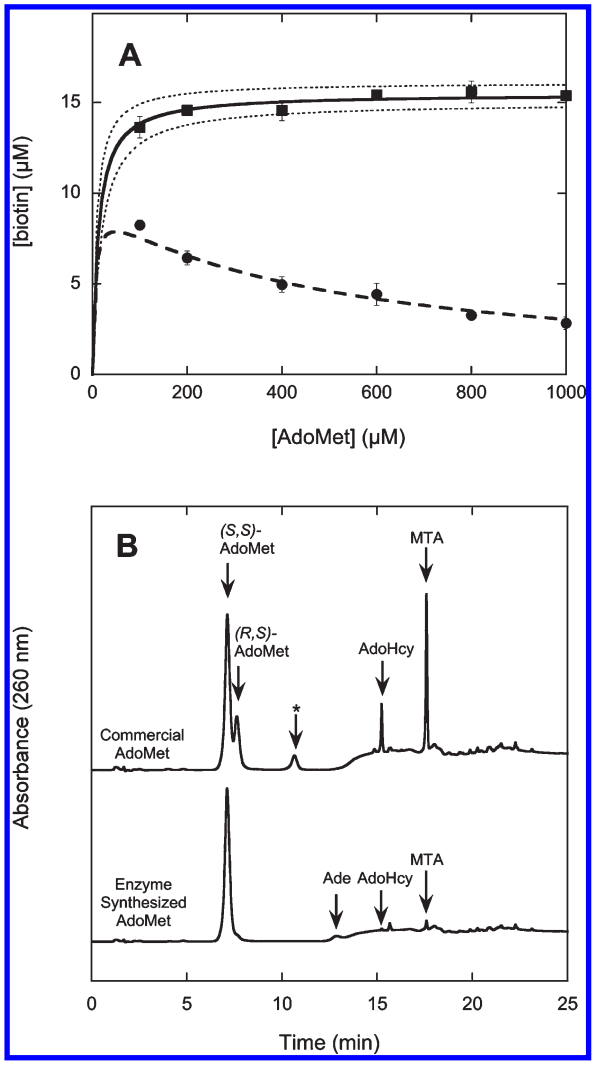

FIGURE 1: Comparison of BS activity using commercial or pure AdoMet. (A) The amount of biotin produced by BS (25 μM) was determined by HPLC analysis following 30 min incubation at 37 °C with DTB (50 μM) and varying concentrations of AdoMet (100−1000 μM), with all other conditions as described for a standard assay. Pure (*S*,*S*)-AdoMet (■), synthesized enzymatically using AdoMet synthetase, exhibited Michaelis−Menten kinetics (V_{max} = 0.52 ± 0.04 μM/min, K_m = 10 ± 5 μM). Dashed curves show fits using K_m values of 6 and 18 μM for comparison. Unpurified commercial AdoMet (●) shows significant inhibition at high concentration and is fit to a model for noncompetitive or cooperative inhibition by a trace contaminant (V_{max} = 0.52 μM/min, K_m = 10 μM, [I]/[S]K_i = 0.002). (B) HPLC analysis of contaminants present in commercial AdoMet (upper trace) and enzymatically synthesized AdoMet (lower trace). The HPLC protocol gives clear separation of AdoMet (t_R = 7.2 min) from the diastereomer (*R*,*S*)-AdoMet (t_R = 7.7 min), adenine (Ade; t_R = 13.0 min), AdoHcy (t_R = 15.3 min), and MTA (t_R = 17.6 min), identified by coinjection with authentic standards. One major contaminant (*) in commercial AdoMet does not coinject with any known AdoMet-related compounds.

inhibition was occurring at high AdoMet concentrations (> 100 μM, Figure 1A, filled circles). This inhibition could be explained by two hypothetical scenarios: (i) BS could be subject to substrate inhibition, with a second weak AdoMet binding site that decreases activity at high concentrations, or (ii) a contaminant in the AdoMet sample could be acting as a noncompetitive or cooperative inhibitor of BS activity. Further purification of the AdoMet sample should distinguish these possibilities, since substrate inhibition would be largely unaffected by the purity of the sample, while inhibition by a contaminant would decrease as the purity is increased.

In order to follow the purification of AdoMet, we developed analytical HPLC conditions that could separate and quantify the various nucleotide contaminants in AdoMet preparations (Figure 1B). By comparison to authentic AdoMet, MTA, adenine, and AdoHcy standards, we observed that typical commercial AdoMet samples contained only ~43% of the biologically active (*S*,*S*)-AdoMet diastereomer, with 25% (*R*,*S*)-AdoMet, 17% MTA, and 5% AdoHcy, as well as ~10% of an unidentified contaminant (Figure 1B, upper trace). AdoMet is enzymatically synthesized in the (*S*,*S*) configuration, where the first designation specifies the chirality of the sulfonium center and the second that of the methionine α-carbon. Racemization at the sulfonium center is spontaneous with $t_{1/2} = 107$ h at 37 °C (*36*). The presence of MTA in the AdoMet samples is due to spontaneous intramolecular S_N2 attack of the methionine carboxylate on the γ-carbon, with expulsion of MTA as the leaving group, occurring spontaneously with $t_{1/2} = 42$ h under physiological conditions (*36*). AdoHcy does not form spontaneously from AdoMet, and the presence in commercial AdoMet preparations is presumably due to incomplete purification of AdoMet derived commercially from yeast cultures.

Cation-exchange chromatography could remove most of the MTA and AdoHcy contaminants but could not remove the unnatural (*R*,*S*)-AdoMet diastereomer. To obtain a stereochemically pure sample of (*S*,*S*)-AdoMet, we used *E. coli* AdoMet synthetase to produce AdoMet, purified this material using weak cation-exchange chromatography followed by lyophilization, and diluted the resulting powder in water to produce a stock solution that was then stored at −80 °C. HPLC analysis indicates this sample contains ≥93% (*S*,*S*)-AdoMet, ≤4% (*R*,*S*)-AdoMet, 2% adenine, 1% MTA, and < 0.1% AdoHcy (Figure 1B, lower trace).

Enzyme-synthesized AdoMet gave an approximately constant level of activity from 100 to 1000 μM AdoMet, with no evidence for inhibition at high AdoMet concentrations. The data are fit to classic Henri−Michaelis−Menten kinetics and are consistent with $K_m^{AdoMet} = 10 \pm 5$ μM and $V_{max} = 0.52$ μM min^{-1} (or $k_{cat} = 0.021$ min^{-1}), similar to the maximum rate of biotin formation in previous studies (*9*, *14*). Since the velocity is nearly saturated at all concentrations, there is considerable uncertainty in the true value for the K_m, and we find that a range of values from 6 to 18 μM is consistent ($R^2 > 0.5$) with the range and the reproducibility of the data (Figure 1A, dotted curves). This uncertainty has implications for the accuracy of the inhibition constants as discussed below.

The inhibition of an enzyme by a trace contaminant in the substrate has been thoroughly examined by Segel (*35*). In general, a purely competitive inhibitor cannot be detected, since the contaminant concentration rises in parallel with the substrate concentration. However, if the inhibition is either noncompetitive or the inhibitor induces strong cooperative effects, then inhibition is detected at high substrate/inhibitor concentrations. Using the K_m^{AdoMet} and V_{max} obtained for enzyme-synthesized AdoMet, we modeled the data obtained for commercial AdoMet to noncompetitive inhibition by a contaminant. Since the contaminant concentration is not known, an explicit K_i cannot be determined, but we can estimate a ratio $x/K_i = 0.002$, where $x = [I]/[AdoMet]$.

Biotin Synthase Is Inhibited by 5′-Deoxyadenosine, AdoHcy, and Sinefungin. Since we could not be certain which of the several contaminants present in commercial AdoMet samples was acting as an inhibitor, we carried out a broad screen of AdoMet-related molecules, as well as BS reaction products and molecules that mimic reaction products (Figure 2). Potential inhibitors were added at a concentration of 500 μM to typical BS activity assays. In some samples, methionine, homocysteine, or

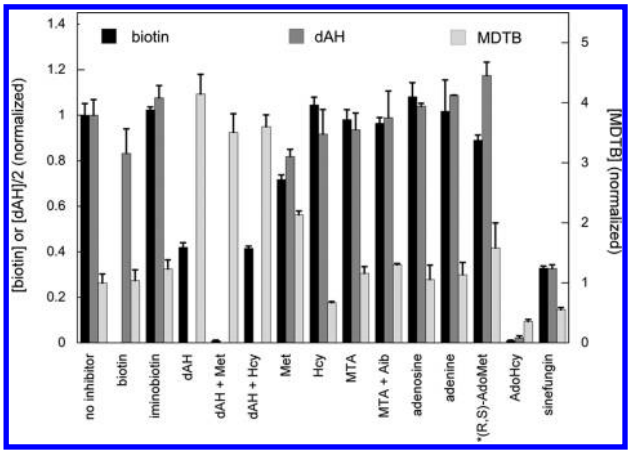

FIGURE 2: Screen for BS inhibition by products and product-related compounds. Potential inhibitors (500 μM) were added to BS (25 μM), DTB (50 μM), and AdoMet (100 μM), with all other conditions as described for a standard assay. Inhibition by (*R*,*S*)-AdoMet was examined by using repurified heat-epimerized AdoMet that contained a mixture of 55 μM (*R*,*S*)-AdoMet and 100 μM (*S*,*S*)-AdoMet. HPLC analysis was used to determine the concentration of the products biotin and dAH (left axis) and the reaction intermediate MDTB (right axis). For samples that contain either biotin or dAH as inhibitors, the amount of that specific product resulting from enzyme turnover could not be determined due to the large excess initially present as an inhibitor, and the data show only the product that could be accurately determined. The data are an average of two measurements and are normalized to the level of product in samples containing no inhibitor.

the nearly isosteric unnatural amino acid 2-aminoisobutyric acid (Aib) was added together with dAH or MTA, with each substance present at 500 μM concentration. Potential inhibition by the unnatural diastereomer (*R*,*S*)-AdoMet was also examined by adding a sample of heat-racemized AdoMet with [(*R*,*S*)-AdoMet] = 55 μM, or approximately 35% of the total AdoMet concentration. Following a 30 min assay at 37 °C, each sample was analyzed by HPLC to determine the concentration of biotin (black bars), dAH (dark gray bars), and MDTB (light gray bars). In cases where either excess biotin or dAH was added as a potential product inhibitor, only the other product was analyzed.

Of the several contaminants present in commercial AdoMet samples, only AdoHcy is a strong inhibitor of BS, with no detectable biotin produced in the presence of 500 μM AdoHcy. MTA is not an inhibitor either by itself or in combination with the complementary isosteric amino acid α-aminoisobutyric acid (Aib). Since we could not obtain a pure sample of (*R*,*S*)-AdoMet, we could only examine potential inhibition by this unnatural diastereomer by producing a sample of heat-racemized AdoMet and comparing activity with this as a substrate as compared to enzyme-synthesized AdoMet. Biotin production is decreased by ~15%, suggesting that (*R*,*S*)-AdoMet could be a modest inhibitor with $K_i \geq 200$ μM, and this inhibition could partially contribute to the decreased activity observed with commercial AdoMet. Under physiologic conditions, (*R*,*S*)-AdoMet spontaneously degrades to MTA and does not significantly accumulate (*36*), and the inhibition of BS observed *in vitro* is not likely to be biologically relevant.

Prior studies have suggested that products of the BS reaction can act as modest inhibitors (*21*). We confirm that dAH and methionine are inhibitors and that this inhibition is amplified when both products are present in equimolar concentration (Figure 2). Homocysteine (Hcy) was not an inhibitor and did not amplify the inhibition by dAH, suggesting that the hydrophobic nature of the methionine thioether, and not the metal-binding capability of the

sulfur, is essential for binding of this amino acid. In contrast to dAH and methionine, neither biotin nor iminobiotin, the guanido analogue of biotin, is a significant inhibitor of BS. In addition, we examined inhibition by the natural product sinefungin, a modified nucleotide structurally related to AdoMet that is a common inhibitor of AdoMet-dependent methyltransferases. We find that sinefungin is also an inhibitor with a decrease in activity comparable to that observed for dAH.

It is interesting to note that for some of the inhibitors the level of biotin is low but the level of the enzyme reaction intermediate, 9-mercaptodethiobiotin (MDTB), is elevated in a 30 min assay (Figure 2). For example, samples containing dAH or dAH/Met have approximately 3−4 times the concentration of MDTB as the control sample. The presence of high levels of intermediate in these samples indicates that AdoMet binds to produce the reaction intermediate during the first half-reaction, but if dAH and Met remain bound to the active site, the second equivalent of AdoMet needed for the second half-reaction cannot access the active site, and the intermediate is not converted to biotin. However, samples containing sinefungin and AdoHcy have less MDTB than the control sample, indicating that these inhibitors prevent binding of the initial equivalent of AdoMet. This complex behavior likely reflects different affinities of inhibitors and substrates for initial and intermediate enzyme states.

Inhibition by AdoHcy Suggests Biotin Synthase Is Half-Site Active. One of the molecules demonstrating the strongest inhibitory effect on biotin production in the inhibitor screen was AdoHcy. In order to quantify the inhibition of BS by AdoHcy in more detail, the initial rate of biotin production was measured as a function of AdoMet concentration (100−500 μM) at several different AdoHcy concentrations (0−50 μM) (Figure 3A). The data exhibit noticeable sigmoidal behavior, particularly under conditions of low substrate/high inhibitor concentrations, suggesting some type of cooperativity between monomers within the BS dimer. In a manner similar to Segel (*34*), we developed a general model and corresponding equation for cooperative inhibition of a dimeric enzyme that includes the potential for cooperative inhibitory effects on K_m and/or k_{cat} (eq 1). In fitting the experimental data, we found two scenarios that could accurately model the data. In one possible scenario, AdoHcy binding to one active site renders the other active site incapable of binding AdoMet (increased K_m or $b \gg 1$ in eq 1). In an alternate scenario, AdoHcy binding to one active site renders both active sites catalytically inactive ($d \approx 0$ in eq 1) due to competition at one site and a severely depressed k_{cat} at the other site. Since we have not obtained evidence for cooperative effects on binding affinity (see Figure 4), we model only the second scenario.

We were able to model inhibition by AdoHcy by fitting the data (Figure 3A) to eq 1 with a, b, $c = 1$ and $d = 0$, yielding $K_i^{AdoHcy} = 650$ nM, while a range of K_i values from 400 to 1200 nM is consistent with the scatter in the data and the uncertainty in the value for K_m^{AdoMet}. This inhibition constant is low compared to the concentration of enzyme and inhibitor used in our activity assays, and at equilibrium under our experimental conditions, most of the inhibitor is bound to the enzyme and not free in solution, thus invalidating one of the basic assumptions required to solve the kinetic equations, that $[I]_{free} \approx [I]_{total}$. Using the graphical method of Dixon (*37*) to estimate the true K_i, we obtain a value of ~160 nM (range from 100 to 500 nM); however, this method assumes simple competitive inhibition and cannot take into account complex cooperative behavior. The true value for K_i^{AdoHcy} is almost certainly less than 650 nM, but in order to accurately determine this value, we would need to develop an enzyme assay in which the enzyme concentration is comparable to or less than K_i.

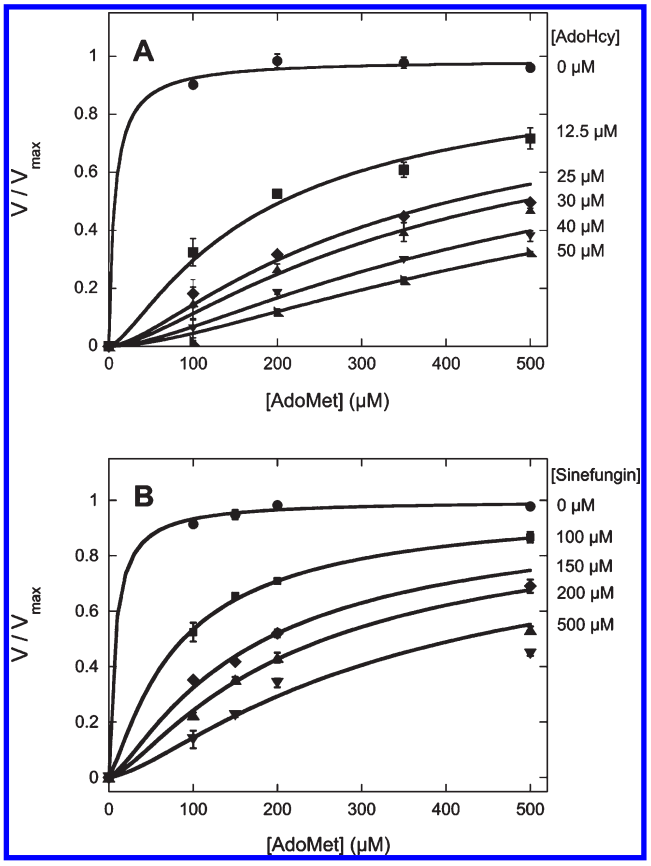

FIGURE 3: Inhibition of BS activity by AdoHcy and sinefungin. The rate of biotin formation by BS (25 μM) was determined in a 30 min assay at 37 °C as described for a standard assay in the Materials and Methods. (A) Inhibition by AdoHcy was examined by varying the concentrations of AdoMet (100, 200, 350, and 500 μM) and AdoHcy (0, 12.5, 25, 30, and 50 μM). The data are fit to eq 1, with a, b, $c = 1$ and $d = 0$, yielding $K_i^{AdoHcy} = 650 \pm 250$ nM and $K_m^{AdoMet} = 10 \pm 5$ μM. (B) Inhibition by sinefungin was examined by varying the concentrations of AdoMet (100, 150, 200, and 500 μM) and sinefungin (0, 250, 500, 750, and 1000 μM). The data are fit to eq 1, with a, b, $c = 1$ and $d = 0$, yielding $K_i^{sinefungin} = 75 \pm 35$ μM and $K_m^{AdoMet} = 10 \pm 5$ μM.

Since AdoHcy inhibits BS in activity assays with such apparent high affinity, we could use this tight-binding inhibitor to titrate the number of active sites within the BS dimer. BS (25 μM monomer) was assayed in the presence of 100 μM AdoMet and increasing concentrations of AdoHcy (0−100 μM). Nearly complete inhibition is accomplished with significantly less than a stoichiometric concentration of AdoHcy (Figure 4A). Extrapolation of the initial linear portion of the inhibition curve indicates that 10.6 μM AdoHcy (0.85 equiv per dimer) is sufficient to completely abolish activity, in agreement with a model in which binding of AdoHcy to one active site renders both active sites within the dimer catalytically inactive.

As noted above, the observed half-site inhibition could have been due to cooperative effects on binding of inhibitor and substrate, which could be examined more directly using equilibrium binding methods. To examine the binding of AdoHcy to BS, we employed a method previously used for determining the dissociation constant of AdoMet, which takes advantage of a decrease in the extinction coefficient in the 350−450 nm region of the UV/visible spectrum when the binding of substrate alters the ligation state or coordination geometry of the $[4Fe\text{-}4S]^{2+}$ cluster in the

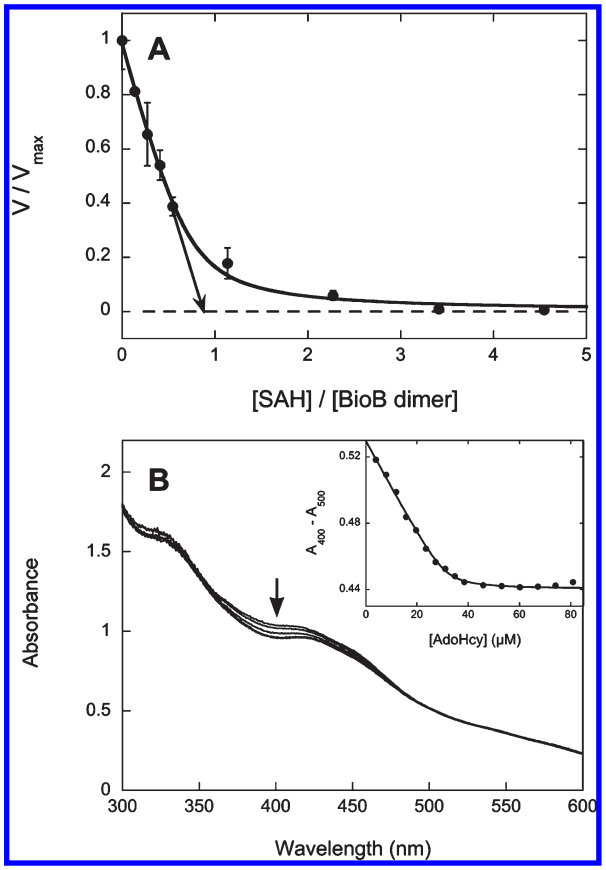

FIGURE 4: Titration of AdoHcy binding sites on BS in the presence of saturating DTB. (A) The concentration of AdoHcy binding sites in the BS dimer that must be filled for complete inhibition was determined in an assay of BS (25 μM monomer) for 30 min at 37 °C. The concentration of AdoHcy was increased from 0 to 100 μM at a constant concentration of the competing substrate AdoMet (100 μM) and an excess of DTB (200 μM). The concentration of biotin produced was determined by HPLC analysis and normalized to the amount produced in the absence of inhibitor; each point represents the average and standard deviation of three trials. Extrapolation of the initial linear decrease in the quadratic inhibition curve yields an active site concentration of 10.6 μM, or 0.85 sites per BS dimer. (B) The total concentration of AdoHcy binding sites in the BS dimer was determined by equilibrium titration in the presence of saturating DTB. BS (50 μM) was reconstituted under argon in a septum-covered cuvette with Na_2S (200 μM) and $FeCl_3$ (200 μM) in 5 mM DTT, 50 mM Tris-HCl, and 100 mM KCl, pH 8.0, and excess DTB (200 μM) was added. AdoHcy (0−100 μM) was added with a syringe, and a UV/visible spectrum was collected following each addition of AdoHcy. Spectra are shown following addition of 0, 10, 20, 40, and 60 μM AdoHcy (from top to bottom trace). The arrow indicates a decrease in absorbance at 400 nm as AdoHcy is added. (Inset) The difference in absorbance between 400 and 500 nm is replotted as a function of added AdoHcy. The concentration of AdoHcy binding sites and the dissociation constant for AdoHcy were determined by fitting these data to eq 3, yielding $K_d^{AdoHcy} = 0.54 \pm 0.15$ μM and [binding sites]/[BS dimer] = 1.5.

enzyme (*33*). An anaerobic solution of reconstituted BS (50 μM) was titrated with AdoHcy (0−100 μM), and UV/visible spectra were recorded after each addition (Figure 4B). The maximum decrease in absorbance was at 400 nm, and there was essentially no absorbance change at 500 nm, and by subtracting these two wavelengths, we could reduce the scatter in the data. The change in absorbance ($\Delta A = A_{400} - A_{500}$) was fit to a quadratic binding isotherm (eq 4), yielding $K_d^{AdoHcy} = 540 \pm 150$ nM and [binding sites] = 37 ± 3 μM (1.5 sites per dimer). The concentration of AdoHcy binding sites may have been slightly lower than the total monomer concentration due to partial oxidative degradation of the $[4Fe\text{-}4S]^{2+}$ cluster during the fairly long titration experiment. A dissociation constant for AdoHcy of 540 nM lies within the range obtained for the inhibition constant and is ~5-fold lower than the K_d = 2.3 μM reported for AdoMet (*33*). Furthermore, we have not observed any evidence for cooperative behavior in equilibrium binding experiments with either AdoMet (*33*) or AdoHcy. Since approximately two binding sites per dimer are observed in equilibrium binding experiments, but only one site must be occupied to completely inhibit the enzyme, this suggests that binding of AdoHcy at one active site induces conformational changes that render the other active site catalytically inactive, despite being fully capable of binding substrate or inhibitor. This observation raises the intriguing question of whether binding of substrates at one active site induces similar conformational changes, which would render the enzyme half-site active.

Sinefungin is a natural product from *Streptomyces incarnatus* in which C3 of ornithine is attached to C5′ of dAH, generating a molecule that is an approximate steric and electrostatic mimic for AdoMet. Sinefungin is an inhibitor of numerous AdoMet-dependent methyltransferases. In order to quantify the inhibition of BS by sinefungin, the initial rate of biotin production was measured as a function of AdoMet concentration (100−500 μM) at several different sinefungin concentrations (0−500 μM) (Figure 3B). The data also exhibit noticeable sigmoidal behavior, particularly under conditions of low substrate/high inhibitor concentrations, suggesting some type of cooperativity between monomers within the BS dimer. In a manner similar to inhibition by AdoHcy, the data are fit to a model in which inhibitor binding to one active site induces conformational changes that render the other active site catalytically inactive ($d \approx 0$ in eq 1). After fitting the sinefungin data to eq 1 using a, b, c = 1 and d = 0, we calculate $K_i^{sinefungin}$ = 75 μM, while a range of K_i values from 40 to 140 μM is consistent with the scatter in the data and the uncertainty in the value for K_m^{AdoMet}.

dAH and Methionine Cooperatively Inhibit BS Activity. Our initial inhibitor screen demonstrated that while both dAH (45% active) and methionine (72% active) are moderate BS inhibitors, the combination of both products in equimolar concentrations resulted in more than simple additive inhibition (< 1% active). This strongly suggests that dAH and methionine bind cooperatively to BS. To measure the cooperative inhibition by dAH and methionine, biotin produced during a BS activity assay was measured in a series of samples in which dAH (0−500 μM) and methionine (0−2000 μM) were varied in parallel, while holding the concentration of the competitive substrate AdoMet constant at 100 μM. dAH alone is a modest inhibitor (Figure 5, top trace) with K_i^{dAH} = 20 μM; however, as methionine is added, the apparent inhibition constant for dAH decreases. The complete set of data was globally fit to a general equation for a cooperative competitive inhibition by two different nonexclusive inhibitors (eq 2), yielding K_i^{Met} = 100 μM and α = 0.3. This latter cooperativity factor is the extent to which the inhibition constant for each inhibitor is altered by the presence of saturating concentrations of the other inhibitor; thus, in the presence of saturating methionine the effective $K_i^{dAH:Met}$ = 6 μM. By comparison, Challand et al. report an IC_{50} = 114 μM for a 1:1 ratio of dAH and methionine (*21*), and assuming they used commercial AdoMet at ~50% purity and using our values for K_m^{AdoMet}, K_i^{Met}, and α, this corresponds to a calculated $K_i^{dAH:Met}$ = 11 μM. However, since their assays were conducted for 3 h (rather than 30 min used in our study), the significant amount of dAH and methionine produced during the assays would result in more apparent inhibition and an erroneously low IC_{50} value. Since dAH is only produced by AdoMet radical enzymes, which are not

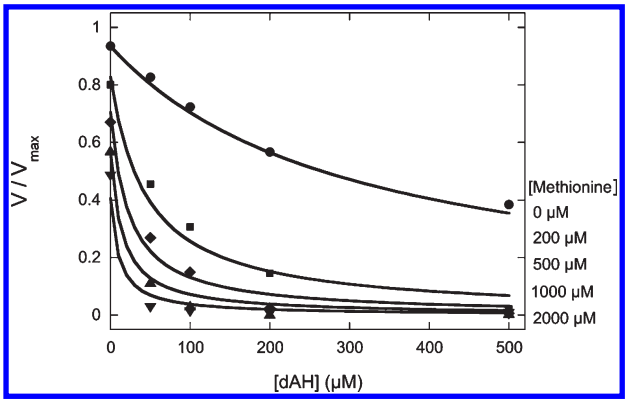

FIGURE 5: Cooperative product inhibition of BS activity by dAH and methionine. The amount of biotin produced by BS (25 μM) was determined by HPLC following incubation for 30 min at 37 °C with DTB (50 μM), AdoMet (100 μM), and dAH and/or Met, with all other conditions as described for a standard assay. Cooperativity of the inhibition by dAH and Met was examined by generating an array of samples with varying concentrations of dAH (50, 100, 200, and 500 μM) and methionine (0, 200, 500, 1000, and 2000 μM). Data are globally fit to eq 2, yielding $K_i^{dAH} = 20 \pm 5\,\mu$M, $K_i^{Met} = 100 \pm 30\,\mu$M, and $\alpha = 0.3$.

Table 1: Kinetic Constants for Alternate MTA Nucleosidase Substrates

substrate	K_m (μM)	k_{cat} (s^{-1})	k_{cat}/K_m ($s^{-1}\,M^{-1}$)
dAH	4.6 ± 0.5	5.1 ± 0.1	$(1.1 \pm 0.1) \times 10^6$
AdoHcy[a]	1.3 ± 0.2	2.6 ± 0.1	$(2.1 \pm 0.3) \times 10^6$
MTA[a]	0.8 ± 0.2	3.0 ± 0.1	$(3.6 \pm 0.7) \times 10^6$

[a]Data for MTA and AdoHcy are reproduced from Lee et al. (*32*).

known to be involved in any major metabolic pathways, the physiologic concentration of dAH is likely to be sufficiently low that *in vivo* product inhibition of BS is probably minimal. However, *in vitro* assays are typically conducted with 10−100 μM enzyme and produce >2 equiv of dAH and methionine, and therefore product inhibition is likely to be a significant factor limiting BS activity, particularly at high enzyme concentrations or prolonged incubation times. Methods for relieving product inhibition might be expected to significantly affect *in vitro* kinetic data.

MTA/AdoHcy Nucleosidase Degrades MTA, AdoHcy, and dAH with Similar Catalytic Efficiency. Prior studies have shown that dAH is an alternate substrate for MTAN (*21*, *22*), and this likely represents the primary degradation pathway for dAH, MTA, and AdoHcy in *E. coli*. To better understand how this enzyme might affect BS activity, we determined the steady-state kinetic constants for dAH reacting with *E. coli* MTA/AdoHcy nucleosidase and compare these to previous results for other substrates obtained under identical assay conditions (Table 1) (*32*). Although dAH has a 5.8- and 1.6-fold weaker affinity for MTA nucleosidase ($K_m^{dAH} = 4.6\ \mu$M) as compared to MTA and AdoHcy, this is compensated by an increase in the turnover rate with dAH ($k_{cat} = 5.1\ s^{-1}$), which is 1.7- and 2-fold faster than with MTA and AdoHcy. The net effect is that dAH, MTA, and AdoHcy are degraded with comparable catalytic efficiency ($k_{cat}/K_m \approx 10^6\ M^{-1}\ s^{-1}$), suggesting that all are degraded in parallel at similar rates in *E. coli*.

MTA/AdoHcy Nucleosidase Increases BS Activity. Since AdoMet preparations are routinely contaminated with AdoHcy and the assay generates significant amounts of dAH, and both are potential BS inhibitors, we sought to relieve this inhibition by degrading these nucleotides using MTAN. To investigate the

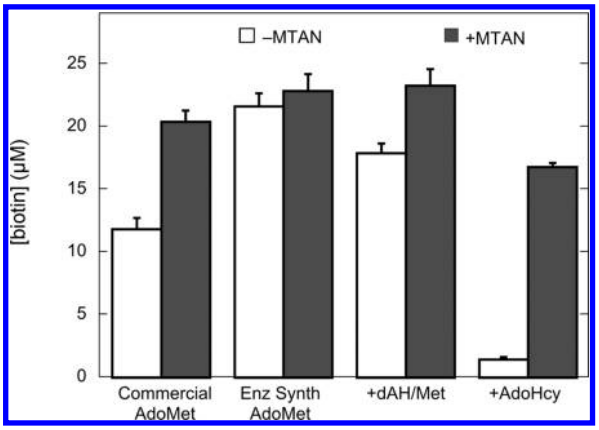

FIGURE 6: Effect of MTA nucleosidase on BS activity. The amount of biotin produced by BS (25 μM) was determined in a standard 30 min assay at 37 °C containing DTB (50 μM) and either AdoMet obtained from commercial sources or enzymatically synthesized AdoMet (200 μM based on A_{260}). In addition, activity assays were also conducted containing enzyme-synthesized AdoMet plus either dAH and methionine (50 μM each) or AdoHcy (50 μM) as inhibitors. Open bars represent biotin produced in assays without the addition of MTAN, and closed bars represent biotin produced in assays to which MTAN (200 nM) was added. Experiments were conducted in triplicate, and error bars represent ±SD.

effect of MTAN on the activity of BS in the presence of inhibitors, MTAN (200 nM) was added to BS (25 μM) and assayed for 60 min at 37 °C with either AdoHcy (50 μM) or dAH and methionine (50 μM each). The biotin produced from these samples was compared to similar samples containing inhibitor but without the addition of MTAN (Figure 6). Additional samples also compared the activity with commercial and enzymatically synthesized AdoMet with and without MTAN. In the absence of MTAN, the assays conducted using commercial AdoMet were only ~50% as active as those conducted using enzymatically synthesized AdoMet, consistent with the results in Figure 1. However, in the presence of MTAN, the activity is similar regardless of the source of AdoMet. The small residual difference in activity could be due to the presence of ~25% (*R*,*S*)-AdoMet in the commercial AdoMet sample, which could be acting as a weak competitive inhibitor that is not degraded by MTAN. When dAH and methionine were added in amounts that would be generated in a typical BS activity assay (50 μM each), the enzyme activity is decreased by ~20%; however, the activity is fully restored upon addition of MTAN. In contrast, when 50 μM AdoHcy is added to a BS activity assay, the activity is decreased by ~95%, and the activity is only partially restored by the addition of MTAN. This residual inhibition by AdoHcy is surprising, given that inhibitor dissociation (estimated at $k_{off} \geq 10\ s^{-1}$) and MTAN turnover ($k_{cat} = 2.6\ s^{-1}$) are both rapid relative to the time scale of the BS assay. One possible explanation that we are exploring is that a portion of the AdoHcy has become oxidized to the sulfoxide, which is not a substrate for MTAN and could be an inhibitor of BS. However, despite this residual inhibition, the data indicate that addition of MTAN to BS assays should relieve most of the inhibition due to contaminating AdoHcy and production of dAH.

BS Undergoes Multiple Turnovers in the Absence of Inhibition. Prior studies of the time course of biotin production by BS have almost certainly been performed with AdoMet contaminated with varying amounts of AdoHcy and, in addition, with varying levels of product inhibition depending on the amount of dAH generated both in the catalytic reaction and due to uncoupled reductive cleavage of AdoMet. Since we found that MTAN could

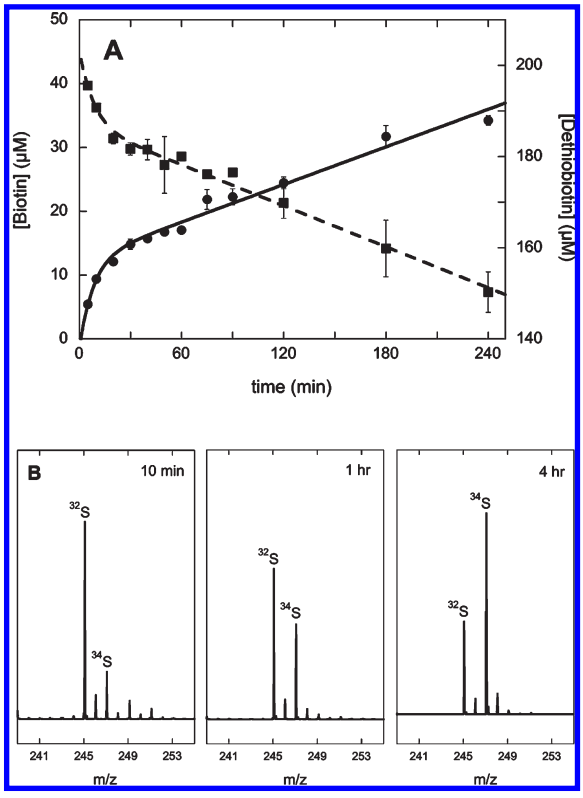

FIGURE 7: BS is half-site active and undergoes slow steady-state turnover. (A) A time course for the formation of biotin (left axis) and consumption of DTB (right axis) at 37 °C in an assay containing BS (22 ± 0.5 μM), AdoMet (200 μM), DTB (200 μM), and MTAN (200 nM), with all other conditions as described for a standard assay. Data were fit to a pre-steady-state burst followed by steady-state turnover (eq 4), yielding the following kinetic constants: [burst] = 11 ± 1 μM, k_{burst} = 0.12 ± 0.03 min^{-1}, and k_{SS} = 0.0089 ± 0.0018 min^{-1}. (B) ESI MS analysis of biotin formed by BS (25 μM) in a standard assay, except with excess $Na_2{}^{34}S$ (800 μM) added to the reaction mixture at t = 0 min. Samples were collected at 10, 60, and 240 min, the reaction was quenched with acid as described for a standard assay, and the biotin was analyzed by ESI MS. ^{32}S-Biotin: [M+ H^+] = 245.1. ^{34}S-Biotin: [M+H^+] = 247.1.

degrade both AdoHcy and dAH, we undertook a reexamination of the optimal *in vitro* activity that could be obtained under strictly anaerobic conditions. BS (22.0 ± 0.5 μM monomer) was reconstituted with Fe^{3+} (200 μM), S^{2-} (200 μM), and DTT (5 mM) and incubated with AdoMet (200 μM) and MTAN (200 nM) in 50 mM Tris-HCl and 100 mM KCl, pH 8.0, for 5 min. The enzymatic reducing system, consisting of flavodoxin (25 μM), ferredoxin: $NADP^+$ oxidoreductase (4 μM), and NADPH (1 mM), was added and the sample incubated for 10 min at 25 °C. Turnover was initiated by adding DTB (200 μM) and transferring the sample to a 37 °C bath, and then samples were periodically removed, quenched with acid, and analyzed by HPLC. Biotin and dAH were produced in a manner that shows a distinct burst over the first 20 min followed by a linear phase that continues to at least 4 h (Figure 7A) and were fit to an equation for burst kinetics (eq 5). This analysis gives a rate constant for biotin formation in the pre-steady-state exponential phase of k_{burst} = 0.12 min^{-1}, which then slows to a turnover number of k_{SS} = 0.0089 min^{-1} during the steady-state phase. The concentration of active sites participating in the burst phase was 11 ± 1 μM, which is the concentration of the dimeric enzyme (not the monomer). This suggests that, at least during the initial rapid burst phase, the BS dimer is half-site active, with only one of the two monomers producing biotin and dAH. The consumption of DTB also shows burst kinetics; however, slightly more DTB is consumed in the burst phase (~13 μM), with the remainder of the consumed DTB found as the MDTB intermediate (not shown), presumably still bound to the enzyme. Assuming that subsequent turnovers also involve a half-site active dimer, then 11 μM BS dimer is producing 35 μM biotin over 4 h, indicating at least three consecutive turnovers. These results were surprising, since BS had not previously been reported to undergo more than one turnover per monomer in an *in vitro* assay.

Biotin formation is accompanied by (or preceded by) destruction of the $[2Fe\text{-}2S]^{2+}$ cluster, presumably providing the sulfur for the biotin thiophane ring, rendering the enzyme inactive after each turnover. In order for additional turnovers to occur, it would presumably be necessary for the $[2Fe\text{-}2S]^{2+}$ cluster to be reconstituted. In order to determine whether additional turnovers involved reconstitution of the $[2Fe\text{-}2S]^{2+}$ cluster using exogenous sulfide, we conducted assays in which BS and the initial $[2Fe\text{-}2S]^{2+}$ cluster contain natural abundance sulfur/sulfide (96% ^{32}S, 4% ^{34}S), while an excess of $Na_2{}^{34}S$ (6% ^{32}S, 94% ^{34}S) was added to the buffer. Preliminary studies had demonstrated that the $[2Fe\text{-}2S]^{2+}$ cluster exchanges only very slowly with $^{34}S^{2-}$ alone, or with Fe^{3+} + $^{34}S^{2-}$ together, when these components are in the buffer and the enzyme is not undergoing catalysis, with ~5−10% exchange over 4 h. If multiple turnovers involve destruction of the initial $[2Fe\text{-}2S]^{2+}$ cluster followed by *in situ* reconstitution of this cluster, then the first turnover should generate ^{32}S-biotin, and all subsequent turnovers should generate ^{34}S-enriched biotin.

As expected, biotin generated during the initial burst phase contains predominantly ^{32}S derived from the initial unlabeled $[2Fe\text{-}2S]^{2+}$ cluster in the aerobically purified protein (81% ^{32}S, 19% ^{34}S after 10 min, Figure 7B). However, as turnover continues, biotin is increasingly generated containing $^{34}S^{2-}$ acquired from the buffer (60% ^{32}S, 40% ^{34}S after 1 h). At later time points, after the first hour, all new biotin is formed utilizing $^{34}S^{2-}$ from the buffer (31% ^{32}S, 69% ^{34}S after 4 h). Surprisingly, a crude analysis of the level of ^{34}S incorporation suggests that all of the ^{32}S found in biotin is derived from the initial burst phase: if the burst generated 11 μM ^{32}S-biotin (from 11 μM BS dimer) and subsequent turnover generated 24 μM ^{34}S biotin, then the 4 h sample would be predicted to contain 66% ^{34}S-biotin. Although several scenarios could explain these results, one possibility is that the conformational changes that render the dimeric enzyme half-site active are very slow to reverse, such that the monomer that has already undergone turnover and now contains a freshly reconstituted FeS cluster is in a more active conformation than the monomer that did not undergo turnover. Clearly, more detailed studies are necessary to critically examine this unprecedented hypothesis.

DISCUSSION

AdoMet is a substrate for numerous nonradical and radical enzymes that utilize each of the three substituents around the sulfonium center, generating both nucleotide and nonnucleotide products (*38*). AdoMet methyltransferases generate AdoHcy as a stoichiometric product and, in addition to the well-recognized nucleotide (*39*) and protein (*40*) methyltransferases, also include enzymes involved in bacterial osmolyte stress response such as glycine, sarcosine, and dimethylglycine methyltransferases (*41*). Cyclopropane fatty acid synthases catalyze nucleophilic attack of an olefin on the methyl group of AdoMet and also generate AdoHcy (*42*). Aminopropyltransferases involved in polyamine biosynthesis and bacterial biofilm formation utilize decarboxylated AdoMet as a source of the aminopropyl group and generate MTA

as a stoichiometric product (*43*), while the recently recognized radical enzyme Dph2, involved in the biosynthesis of dipthamide during ribosome maturation, utilizes AdoMet as a source of a 3-carboxy-3-aminopropyl group and also generates MTA (*44*). Numerous AdoMet radical enzymes utilize AdoMet as an oxidant and generate dAH as a stoichiometric product (*45*, *46*). As might be expected, AdoHcy, MTA, and dAH act as product inhibitors of the respective enzymes that generate these nucleotides, as well as other AdoMet-dependent enzymes, and recycling pathways are important not only in maintaining a balanced nucleotide pool but also in relieving enzyme inhibition.

Numerous studies have quantitatively examined product inhibition of AdoMet methyltransferases by AdoHcy. For example, *E. coli* cytosine 5-methyltransferase is inhibited by AdoHcy with a K_i = 14 μM (*47*), while rat catechol *O*-methyltransferase is inhibited with a K_i = 50 μM (*48*). Aside from methyltransferases, AdoHcy has not been widely reported as an inhibitor of other AdoMet-dependent enzymes, and the inhibition of the AdoMet radical enzymes by AdoHcy has been only briefly mentioned in the literature. Reichard and co-workers reported that AdoHcy inhibits the activation of pyruvate formate-lyase (PFL) by PFL activase with an $IC_{50} \approx 20$ μM at 100 μM AdoMet (*49*); using a subsequently reported K_m^{AdoMet} = 2.8 μM (*50*), this translates to a $K_i^{AdoHcy} \approx 550$ nM. Binding of AdoHcy to lysine 2,3-aminomutase has been documented by perturbation of the $[4Fe\text{-}4S]^+$ cluster EPR spectrum and oxidation−reduction potential (*51*, *52*), and although inhibition was not directly discussed, AdoHcy is presumably a competitive inhibitor of the catalytic reaction. BS is inhibited with comparable high affinity to PFL activase, with $K_i \leq$ 650 nM, and AdoHcy behaves as a nearly stoichiometric tight-binding inhibitor at high enzyme concentrations. For example, assuming AdoHcy is typically a 2−5% contaminant in commercial AdoMet and binding of 1 equiv of AdoHcy per dimer renders BS inactive, then a typical assay run with 25 μM BS (12.5 μM dimer) and 500 μM AdoMet will initially have 6−12 μM inactive BS:AdoHcy complex and only 0.5−6.5 μM free active BS. In light of this analysis, many prior catalytic and spectroscopic studies of BS should be reexamined with a critical eye toward the possibility that the data were influenced by AdoHcy binding and inhibition. Furthermore, the relatively low activity often observed with other AdoMet radical enzymes could be due to contaminating AdoHcy in commercial AdoMet samples. Further purification of AdoMet by cation-exchange chromatography, or the inclusion of AdoHcy hydrolase or MTAN in assay mixtures, should become standard practice when working with AdoMet radical enzymes.

As Roach and co-workers have previously shown (*21*), BS is inhibited by its products dAH and methionine. In the present work, we demonstrate that while dAH (K_i = 20 μM) and methionine (K_i = 100 μM) will each bind and inhibit BS, dAH will also bind cooperatively with methionine, resulting in a 3-fold enhancement of inhibition. However, in a typical BS assay, inhibition is relatively weak and will only occur at high enzyme concentration and at prolonged reaction times when the enzyme has produced greater than stoichiometric amounts of product. For example, an assay that contains 25 μM BS monomer and 100 μM AdoMet will produce ~12.5 μM biotin and ~25 μM dAH and methionine after 1 h, and the remainder of the enzyme will therefore be product inhibited and behave as if it is ~85% active. This modest effect would be somewhat exacerbated at higher BS concentrations, at longer incubation times, or in the presence of AdoHcy. Addition of MTAN to assays would relieve both dAH and AdoHcy inhibition, while methionine inhibition alone is sufficiently weak that it would not influence typical activity assays. In *E. coli*, AdoHcy and dAH are presumably maintained at concentrations below the respective MTAN K_m values of 1.3 and 4.6 μM, respectively, and *in vivo* inhibition of BS would normally be relatively minor.

An *E. coli* deletion mutant lacking the gene encoding MTAN (Δ*pfs*) shows growth retardation that is restored by the addition of biotin and lipoic acid (*22*). A recent study examined AdoMet and AdoHcy levels in WT and Δ*mtn E. coli* strains during exponential growth and stationary phases (*53*) and reports that AdoHcy levels increase from ~1 μM in WT to ~50 μM in the Δ*mtn* strain during exponential growth, while AdoMet levels decrease from ~300 to ~100 μM. These concentration changes would be predicted to result in a 95% decrease in activity of BS. AdoHcy can be rapidly produced *in vivo* through the activity of numerous AdoMet-dependent methyltransferases, and although many organisms have more than one enzyme to metabolize AdoHcy, *E. coli* has only MTAN (*54*). We would suggest that one consequence of mutations in or inhibition of MTAN (or eukaryotic AdoHcy hydrolase) could be subsequent widespread inhibition of AdoMet radical enzymes due to a buildup of AdoHcy. Since biotin and lipoic acid supplementation were sufficient to restore WT growth of a Δ*mtn* mutant, then this would suggest that BS and lipoyl synthase are the only AdoMet radical enzymes important for aerobic growth of *E. coli* in M9-glucose minimal media.

Sinefungin is a potent inhibitor of DNA methyltransferases, binding cooperatively with DNA to give K_i values on the order of 10 nM (*55*). Sinefungin is only a moderate inhibitor of BS, with K_i = 75 μM. However, inhibition by both sinefungin and AdoHcy exhibit informative cooperative effects at low AdoMet concentrations. Since equilibrium binding of AdoHcy or AdoMet (*33*) does not show cooperative effects, we believe that the observed cooperativity is an effect on k_{cat}. A titration of BS activity with increasing concentrations of AdoHcy demonstrates that only 1 equiv of inhibitor per BS dimer will inhibit both active sites within the dimer. One simple interpretation that is consistent with the data is that when the dimeric enzyme has an inhibitor bound in one active site, the other active site becomes catalytically inactive despite being able to bind substrate or inhibitor, consistent with a model for a half-site active dimeric enzyme.

When MTAN is added to BS assays to degrade any initially contaminating AdoHcy and any subsequently produced dAH, DTB consumption and biotin production by BS follow classic burst kinetics (Figure 7). The amplitude of the burst phase is exactly equivalent to the dimer concentration, suggesting that only one active site per dimer can produce biotin with a rate constant of k_{burst} = 0.12 min^{-1}, while the other active site is rendered catalytically inactive. Again, this suggests that the dimeric enzyme is half-site active. The crystal structure of BS (*56*) offers a few clues as to how this cooperativity might be transmitted. The dimer interface consists of a four-helix bundle that is connected to several active site residues via two short loop regions (residues 232−238 and 262−269), and the adenine ring of AdoMet is in a nearby hydrophobic pocket that is partially created by these loops. Perhaps binding of AdoMet to one active site is transmitted through the four-helix bundle to the other active site and causes a rearrangement of these loop residues, such that AdoMet is no longer bound in sufficiently close proximity to the $[4Fe\text{-}4S]^{2+}$ cluster.

Following the burst phase, both DTB consumption and biotin production continue in what appears to be linear steady-state turnover. However, the rate of turnover (k_{SS} = 0.0089 min^{-1}) is significantly slower than the burst phase, suggesting that a step

that follows biotin formation within the active site is now rate-limiting. Prior studies have demonstrated that biotin formation is accompanied by loss of the $[2Fe\text{-}2S]^{2+}$ cluster (*12*−*14*), and if this cluster is the essential sulfur donor, this should render the enzyme catalytically inactive. Thus the rate-limiting step in steady-state turnover is likely to be spontaneous reassembly of the $[2Fe\text{-}2S]^{2+}$ cluster with Fe^{3+} and S^{2-} from the buffer. Consistent with this hypothesis, addition of $^{34}S^{2-}$ to the buffer results in ^{34}S-biotin being formed predominantly in the steady-state phase but not in the burst phase. Further studies are necessary to demonstrate that this labeled sulfur is first assembled into a new $[2Fe\text{-}2S]^{2+}$ cluster before being transferred into biotin.

In vivo, BS has been reported to produce 20−60 molecules of biotin per monomer (*22*) with a turnover rate of ~0.1 min^{-1}. This rate is comparable to the rate of the burst phase observed *in vitro*, suggesting that *in vivo* activity is not limited by FeS cluster reassembly but rather by the chemistry of biotin formation. In *E. coli*, FeS cluster reassembly is catalyzed by proteins from the Isc and/or Suf cluster assembly systems, which, for the most part, have not been kinetically characterized. However, the cysteine desulfurase IscS from the Isc system has a maximal turnover number of 8 min^{-1} (*57*), suggesting that it could provide sulfur for FeS cluster assembly at a rate ~80-fold faster than BS turnover, and therefore FeS cluster assembly is not likely to be rate-limiting. Further enhancement of *in vitro* biotin formation by BS is likely to come about only through improvements in FeS cluster reassembly, possibly by addition of Isc or Suf proteins to the complex enzyme cocktail.

REFERENCES

1. Escalletes, F., Florentin, D., Tse Sum Bui, B., Lesage, D., and Marquet, A. (1999) Biotin synthase mechanism: evidence for hydrogen transfer from the substrate into deoxyadenosine. *J. Am. Chem. Soc. 121*, 3571–3578.
2. Farrar, C. E., and Jarrett, J. T. (2009) Protein residues that control the reaction trajectory in *S*-adenosylmethionine radical enzymes: mutagenesis of asparagine 153 and aspartate 155 in *Escherichia coli* biotin synthase. *Biochemistry 48*, 2448–2458.
3. Guianvarc'h, D., Florentin, D., Tse Sum Bui, B., Nunzi, F., and Marquet, A. (1997) Biotin synthase, a new member of the family of enzymes which uses *S*-adenosylmethionine as a source of deoxyadenosyl radical. *Biochem. Biophys. Res. Commun. 236*, 402–406.
4. Ollagnier-de Choudens, S., Sanakis, Y., Hewiston, K. S., Roach, P., and Munck, E. (2002) Reductive cleavage of *S*-adenosylmethionine by biotin synthase from *Escherichia coli*. *J. Biol. Chem. 277*, 13449–13454.
5. Shaw, N. M., Birch, O. M., Tinschert, A., Venetz, V., Dietrich, R., and Savoy, L. A. (1998) Biotin synthase from *Escherichia coli*: isolation of an enzyme-generated intermediate and stoichiometry of *S*-adenosylmethionine use. *Biochem. J. 330*, 1079–1085.
6. Tse Sum Bui, B., Lotierzo, M., Escalettes, F., Florentin, D., and Marquet, A. (2004) Further investigation on the turnover of *Escherichia coli* biotin synthase with dethiobiotin and 9-mercaptodethiobiotin as substrates. *Biochemistry 43*, 16432–16441.
7. Marquet, A., Florentin, D., Ploux, O., and Tse Sum Bui, B. (1998) *In vivo* formation of C-S bonds in biotin. An example of radical chemistry under reducing conditions. *J. Phys. Org. Chem. 11*, 529–535.
8. Marquet, A., Tse Sum Bui, B., and Florentin, D. (2001) Biosynthesis of biotin and lipoic acid. *Vitam. Horm. 61*, 51–101.
9. Taylor, A. M., Farrar, C. E., and Jarrett, J. T. (2008) 9-Mercaptodethiobiotin is formed as a competent catalytic intermediate by *Escherichia coli* biotin synthase. *Biochemistry 47*, 9309–9317.
10. Baldet, P., Gerbling, H., Axiotis, S., and Douce, R. (1993) Biotin biosynthesis in higher plant cells. Identification of intermediates. *Eur. J. Biochem. 217*, 479–485.
11. Trainor, D. A., Parry, R. J., and Gitterman, A. (1980) Biotin biosynthesis. 2. Stereochemistry of sulfur introduction at C-4 of dethiobiotin. *J. Am. Chem. Soc. 102*, 1467–1468.
12. Jameson, G. N., Cosper, M. M., Hernandez, H. L., Johnson, M. K., and Huynh, B. H. (2004) Role of the [2Fe-2S] cluster in recombinant *Escherichia coli* biotin synthase. *Biochemistry 43*, 2022–2031.
13. Tse Sum Bui, B., Benda, R., Schunemann, V., Florentin, D., Trautwein, A. X., and Marquet, A. (2003) Fate of the $(2Fe\text{-}2S)^{2+}$ cluster of *Escherichia coli* biotin synthase during the reaction: a Mössbauer characterization. *Biochemistry 42*, 8791–8798.
14. Ugulava, N. B., Sacanell, C. J., and Jarrett, J. T. (2001) Spectroscopic changes during a single turnover of biotin synthase: destruction of a [2Fe-2S] cluster accompanies sulfur insertion. *Biochemistry 40*, 8352–8358.
15. Muhlenhoff, U., Gerber, J., Richhardt, N., and Lill, R. (2003) Components involved in assembly and dislocation of iron-sulfur clusters on the scaffold protein Isu1p. *EMBO J. 22*, 4815–4825.
16. Reyda, M. R., Fugate, C. J., and Jarrett, J. T. (2009) A complex between biotin synthase and the iron-sulfur cluster assembly chaperone HscA that enhances *in vivo* cluster assembly. *Biochemistry 48*, 10782–10792.
17. Choi-Rhee, E., and Cronan, J. E. (2005) Biotin synthase is catalytic *in vivo*, but catalysis engenders destruction of the protein. *Chem. Biol. 12*, 461–468.
18. Farrar, C. E., and Jarrett, J. T. (2007) Radical *S*-adenosylmethionine (SAM) superfamily, in Encyclopedia of the Life Sciences, John Wiley & Sons, Chichester, U.K. (http://www.els.net/).
19. Jarrett, J. T. (2003) The generation of 5′-deoxyadenosyl radicals by adenosylmethionine-dependent radical enzymes. *Curr. Opin. Chem. Biol. 7*, 174–182.
20. Ollagnier-de Choudens, S., Mulliez, E., and Fontecave, M. (2002) The PLP-dependent biotin synthase from *Escherichia coli*: mechanistic studies. *FEBS Lett. 532*, 465–468.
21. Challand, M. R., Ziegert, T., Douglas, P., Wood, R. J., Kriek, M., Shaw, N. M., and Roach, P. L. (2009) Product inhibition in the radical *S*-adenosylmethionine family. *FEBS Lett. 583*, 1358–1362.
22. Choi-Rhee, E., and Cronan, J. E. (2005) A nucleosidase required for *in vivo* function of the *S*-adenosyl-L-methionine radical enzyme, biotin synthase. *Chem. Biol. 12*, 589–593.
23. Lee, J. E., Cornell, K. A., Riscoe, M. K., and Howell, P. L. (2001) Expression, purification, crystallization and preliminary X-ray analysis of *Escherichia coli* 5′-methylthioadenosine/*S*-adenosylhomocysteine nucleosidase. *Acta Crystallogr., Sect. D: Biol. Crystallogr. 57*, 150–152.
24. Ugulava, N. B., Gibney, B. R., and Jarrett, J. T. (2000) Iron-sulfur cluster interconversions in biotin synthase: dissociation and reassociation of iron during conversion of [2Fe-2S] to [4Fe-4S] clusters. *Biochemistry 39*, 5206–5214.
25. Ugulava, N. B., Gibney, B. R., and Jarrett, J. T. (2001) Biotin synthase contains two distinct iron-sulfur cluster binding sites: chemical and spectroelectrochemical analysis of iron-sulfur cluster interconversions. *Biochemistry 40*, 8343–8351.
26. Markham, G. D., DeParasis, J., and Gatmaitan, J. (1984) The sequence of *metK*, the structural gene for *S*-adenosylmethionine synthetase in *Escherichia coli*. *J. Biol. Chem. 259*, 14505–14507.
27. Takusagawa, F., Kamitori, S., Misaki, S., and Markham, G. D. (1996) Crystal structure of *S*-adenosylmethionine synthetase. *J. Biol. Chem. 271*, 136–147.
28. Markham, G. D., Hafner, E. W., Tabor, C. W., and Tabor, H. (1980) *S*-Adenosylmethionine synthetase from *Escherichia coli*. *J. Biol. Chem. 255*, 9082–9092.
29. Park, J., Tai, J., Roessner, C. A., and Scott, A. I. (1996) Enzymatic synthesis of *S*-adenosyl-L-methionine on the preparative scale. *Bioorg. Med. Chem. 4*, 2179–2185.
30. Walsby, C. J., Hong, W., Broderick, W. E., Cheek, J., Ortillo, D., Broderick, J. B., and Hoffman, B. M. (2002) Electron-nuclear double resonance spectroscopic evidence that *S*-adenosylmethionine binds in contact with the catalytically active $[4Fe\text{-}4S]^{+}$ cluster of pyruvate formate-lyase activating enzyme. *J. Am. Chem. Soc. 124*, 3143–3151.
31. Dunn, S. M., Bryant, J. A., and Kerr, M. W. (1994) A simple spectrophotometric assay for plant 5-deoxy-5-methylthioadenosine nucleosidase using xanthine oxidase as a coupling enzyme. *Phytochem. Anal. 5*, 286–290.
32. Lee, J. E., Luong, W., Huang, D. J., Cornell, K. A., Riscoe, M. K., and Howell, P. L. (2005) Mutational analysis of a nucleosidase involved in quorum-sensing autoinducer-2 biosynthesis. *Biochemistry 44*, 11049–11057.
33. Ugulava, N. B., Frederick, K. K., and Jarrett, J. T. (2003) Control of adenosylmethionine-dependent radical generation in biotin synthase: a kinetic and thermodynamic analysis of substrate binding to active and inactive forms of BioB. *Biochemistry 42*, 2708–2719.

34. Segel, I. H. (1975) Enzyme Kinetics, pp 389−390, John Wiley & Sons, New York.
35. Segel, I. H. (1975) Enzyme Kinetics, pp 147−150, John Wiley & Sons, New York.
36. Hoffman, J. L. (1986) Chromatographic analysis of the chiral and covalent instability of *S*-adenosyl-L-methionine. *Biochemistry 25*, 4444–4449.
37. Dixon, M. (1972) The graphical determination of K_m and K_i. *Biochem. J. 129*, 197–202.
38. Fontecave, M., Atta, M., and Mulliez, E. (2004) *S*-adenosylmethionine: nothing goes to waste. *Trends Biochem. Sci. 29*, 243–249.
39. Bheemanaik, S., Reddy, Y. V., and Rao, D. N. (2006) Structure, function and mechanism of exocyclic DNA methyltransferases. *Biochem. J. 399*, 177–190.
40. Clarke, S. (1993) Protein methylation. *Curr. Opin. Cell Biol. 5*, 977–983.
41. Kimura, Y., Kawasaki, S., Yoshimoto, H., and Takegawa, K. (2010) Glycine betaine biosynthesized from glycine provides an osmolyte for cell growth and spore germination during osmotic stress in *Myxococcus xanthus*. *J. Bacteriol. 192*, 1467–1470.
42. Iwig, D. F., Grippe, A. T., McIntyre, T. A., and Booker, S. J. (2004) Isotope and elemental effects indicate a rate-limiting methyl transfer as the initial step in the reaction catalyzed by *Escherichia coli* cyclopropane fatty acid synthase. *Biochemistry 43*, 13510–13524.
43. Ikeguchi, Y., Bewley, M. C., and Pegg, A. E. (2006) Aminopropyltransferases: function, structure and genetics. *J. Biochem. 139*, 1–9.
44. Zhang, Y., Zhu, X., Torelli, A. T., Lee, M., Dzikovski, B., Koralewski, R. M., Wang, E., Freed, J., Krebs, C., Ealick, S. E., and Lin, H. (2010) Diphthamide biosynthesis requires an organic radical generated by an iron-sulphur enzyme. *Nature 465*, 891–896.
45. Frey, P. A., and Booker, S. J. (2001) Radical mechanisms of *S*-adenosylmethionine-dependent enzymes. *Adv. Protein Chem. 58*, 1–45.
46. Wang, S. C., and Frey, P. A. (2007) *S*-Adenosylmethionine as an oxidant: the radical SAM superfamily. *Trends Biochem. Sci. 32*, 101–110.
47. Crooks, P. A., Tribe, M. J., and Pinney, R. J. (1984) Inhibition of bacterial DNA cytosine-5-methyltransferase by *S*-adenosyl-L-homocysteine and some related compounds. *J. Pharm. Pharmacol. 36*, 85–89.
48. Coward, J. K., and Slisz, E. P. (1973) Analogs of *S*-adenosylhomocysteine as potential inhibitors of biological transmethylation. Specificity of the *S*-adenosylhomocysteine binding site. *J. Med. Chem. 16*, 460–463.
49. Harder, J., Eliasson, R., Pontis, E., Ballinger, M. D., and Reichard, P. (1992) Activation of the anaerobic ribonucleotide reductase from *Escherichia coli* by *S*-adenosylmethionine. *J. Biol. Chem. 267*, 25548–25552.
50. Wong, K. K., Murray, B. W., Lewisch, S. A., Baxter, M. K., Ridky, T. W., Ulissi-DeMario, L., and Kozarich, J. W. (1993) Molecular properties of pyruvate formate-lyase activating enzyme. *Biochemistry 32*, 14102–14110.
51. Hinckley, G. T., and Frey, P. A. (2006) Cofactor dependence of reduction potentials for $[4Fe\text{-}4S]^{2+/1+}$ in lysine 2,3-aminomutase. *Biochemistry 45*, 3219–3225.
52. Lieder, K. W., Booker, S., Ruzicka, F. J., Beinert, H., Reed, G. H., and Frey, P. A. (1998) *S*-Adenosylmethionine-dependent reduction of lysine 2,3-aminomutase and observation of the catalytically functional iron-sulfur centers by electron paramagnetic resonance. *Biochemistry 37*, 2578–2585.
53. Halliday, N. M., Hardie, K. R., Williams, P., Winzer, K., and Barrett, D. A. (2010) Quantitative liquid chromatography-tandem mass spectrometry profiling of activated methyl cycle metabolites involved in LuxS-dependent quorum sensing in *Escherichia coli*. *Anal. Biochem. 403*, 20–29.
54. Lee, J. E., Settembre, E. C., Cornell, K. A., Riscoe, M. K., Sufrin, J. R., Ealick, S. E., and Howell, P. L. (2004) Structural comparison of MTA phosphorylase and MTA/AdoHcy nucleosidase explains substrate preferences and identifies regions exploitable for inhibitor design. *Biochemistry 43*, 5159–5169.
55. Reich, N. O., and Mashhoon, N. (1990) Inhibition of EcoRI DNA methylase with cofactor analogs. *J. Biol. Chem. 265*, 8966–8970.
56. Berkovitch, F., Nicolet, Y., Wan, J. T., Jarrett, J. T., and Drennan, C. L. (2004) Crystal structure of biotin synthase, an *S*-adenosylmethionine-dependent radical enzyme. *Science 303*, 76–79.
57. Urbina, H. D., Silberg, J. J., Hoff, K. G., and Vickery, L. E. (2001) Transfer of sulfur from IscS to IscU during Fe/S cluster assembly. *J. Biol. Chem. 276*, 44521–44526.